coatings

MDPI

Article

Microstructure Evolution Behavior of Blast-Furnace Coke under Different Gasification Reaction Conditions

Hongliang Wu [1,2], Laihao Yu [1], Shengchao Chang [1], Yingyi Zhang [1,*] and Jialong Yang [1,*]

[1] School of Metallurgical Engineering, Anhui University of Technology, Maanshan 243002, China
[2] Maanshan Iron & Steel Co., Ltd., Maanshan 243003, China
* Correspondence: zhangyingyi@ahut.edu.cn (Y.Z.); jialongyang@126.com (J.Y.)

Abstract: With the development of large-scale blast-furnace and oxygen-rich coal-injection technology, as well as national green and low-carbon policy requirements, the ironmaking process has increasingly strict requirements for blast-furnace raw materials, such as new and higher requirements for coke quality and thermal performance. In this study, the melting loss reaction in a blast furnace was simulated under laboratory conditions and the microstructure evolution of coke after melting loss under CO_2 and $CO_2 + H_2O$ conditions was studied. The results showed that under a CO_2 atmosphere, the specific surface area and pore volume of coke and the number of micropores in coke first increased and then decreased with the increase in reaction time, while the average pore size first decreased from 17.289 to 8.641 nm and then increased to 9.607 nm. In the gasification reaction between CO_2 and coke, the relative content of the graphitized structure (I_G/I_{All}) increased first, then decreased and then increased with the increase in reaction time, while the change trends of disordered structure (I_{D3}/I_G) and unstable structure (I_{D4}/I_G) were opposite to I_G/I_{All}, indicating that coke still tended to be more orderly with the increase in time. In the mixed atmosphere of CO_2 and H_2O, the specific surface area and I_G/I_{All} of coke increased with the increase in H_2O content. However, when the proportion of H_2O exceeded 50%, the specific surface area decreased slightly, and the pore-size value corresponding to the peak value in the pore-size distribution curve shifted to the right, and the average pore-size increased in the nanosize range.

Keywords: blast-furnace coke; micromorphology; pore-size distribution; physicochemical structure

Citation: Wu, H.; Yu, L.; Chang, S.; Zhang, Y.; Yang, J. Microstructure Evolution Behavior of Blast-Furnace Coke under Different Gasification Reaction Conditions. *Coatings* **2022**, *12*, 1116. https://doi.org/10.3390/coatings12081116

Academic Editor: Sigitas Tamulevičius

Received: 20 July 2022
Accepted: 3 August 2022
Published: 4 August 2022

1. Introduction

With the rapid development of technology and the increasing shortage of coking coal resources, many non-blast-furnace ironmaking processes based on melting reduction have emerged in an endless stream at home and abroad [1–3]. Although a number of non-blast-furnace ironmaking technologies have been perfected and matured and have achieved production, blast-furnace ironmaking has a history of more than 100 years, and with the continuous progress of technology, blast-furnace ironmaking is also approaching automation, large scale and high efficiency, so it still has obvious competitive advantages [4–7]. However, under the long-term goal of low pollution, low cost and low consumption, the utilization efficiency of blast-furnace energy must be improved in order to maintain the competitive advantage of blast-furnace ironmaking for a long time [8]. With the rapid development of China's iron and steel industry and the irreplaceability of blast-furnace coke, the demand for coke is increasing. At present, domestic coke used in the iron and steel industry accounts for more than 80% of all coke consumption. Under such a huge user base, in order to achieve the goal of "carbon peaking and carbon neutralization", it is necessary to clarify the evolution process of coke in the blast furnace from the source, and reasonably control the performance of coke, reduce costs and reduce pollution on the premise that the blast furnace is running smoothly [9–12].

The coke in the blast furnace fell from top to bottom through the block zone, soft melting zone, dripping zone and finally to the tuyere cyclotron zone, causing melting loss.

In the whole process, due to the complex internal environment of the blast furnace, coke underwent various thermal stresses and chemical processes, resulting in significant loss and deterioration of its own performance and structure [13,14]. However, the normal operation of the raceway requires coke to maintain a certain quality and lumpiness. Therefore, it is of great significance to analyze the entire coke deterioration process and reduce the carbon melting loss in the decline process, so as to maintain good thermal strength of coke and meet the needs of the dropping zone on the coke skeleton effect for the smooth running and operation of the blast furnace [15].

As one of the main reasons for coke deterioration, the carbon melting reaction mainly refers to the reaction of coke with CO_2 and H_2O. In essence, the carbon melting reaction between coke and CO_2 is an indirect reduction reaction between CO in furnace gas and iron oxide in iron ore, generating a large amount of CO_2, while CO_2 and coke continue to react to generate CO [16–18]. The reaction type is solid–gas reaction: when the gas makes contact with coke, the gas reacts on the coke surface, forming a large number of micropores, and the products diffuse from the inside of the coke to the outside surface through pores [19]. The product of the coke melting-loss reaction is still gas, and the porosity of coke is large, so the reaction between gas and coke can be carried out inside coke [20]. All these behaviors make the coke structure loose and deteriorate. Both temperature and pressure have a certain influence on the coke melting reaction. The research results show that the higher the temperature, the higher the coke reactivity [21], whereas the high-pressure conditions will inhibit the gasification reaction of coke. The carbon melting reaction between coke and H_2O is actually a water–gas reaction. With the increasing H_2 content in coal gas, the water–gas reaction has also attracted much attention. Zhao et al. [22] used cylindrical coke to study the details of the melting-loss reaction between coke and CO_2 and H_2O at 900–1100 °C, respectively. The results showed that the main gasification modes of CO_2, H_2O and coke were micropore generation and small pore expansion at 900 °C, respectively; at 1100 °C, there was small pore expansion and micropore formation, respectively; again, the reaction rate of H_2O was about 2–5 times that of CO_2 at the same temperature, indicating that CO_2 and H_2O had different effects on the degradation behavior and rate of coke.

Since the second half of the 20th century, blast furnaces have gradually begun to implement high air temperature, oxygen-rich blasts, tuyere fuel injection and other measures; this series of highly enhanced smelting processes has led to more intense gasification reactions of coke in blast furnaces. Therefore, it is necessary for scholars to study the differences in microstructure characteristics of coke before and after intense gasification reaction more extensively and deeply, such as stomatal structure, crystal structure and microscopic morphology [23,24]. This research simulated the internal gasification conditions of the blast furnace by adjusting the type and proportion of gas; carried out gasification reaction tests on coke; revealed the evolution trend of micropore distribution, microcrystalline structure and micromorphology of coke in the mixed atmosphere of CO_2 and CO_2 + H_2O; and sought the melting and degradation mechanism of coke from the micro perspective, so as to provide a theoretical basis for improving the performance of coke.

2. Experimental Procedure

2.1. Pretreatment of Coke

The coke used in this experiment is MG 2# furnace coke, and the radius of 2# blast furnace hearth is 5.5 m. Considering that the reaction in the tuyere area of the blast furnace is complex and intense, and the samples are mixed with pellets, fluxes, etc., a certain amount of slag iron will be attached to the coke surface. Therefore, before the study and analysis of blast furnace coke samples, it is necessary to remove the slag iron on the surface of coke samples to avoid affecting the experimental results. Again, the determination of Raman spectrum requires grinding coke samples to $\leq$200 mesh, so the closed prototype is generally used for grinding sample preparation. In addition, the coke samples should be inlaid and polished to create an observable smooth plane before using scanning electron microscope to observe the micromorphology.

2.2. High-Temperature Melting-Loss Test of Coke

It is well known that high-temperature and high-pressure oxidation environment can easily lead to material failure [25–28]. Severe coke melting loss will increase coke porosity, reduce coke mechanical properties and deteriorate the permeability of blast furnace. Therefore, this study used the coke metallurgical performance tester to measure the melting loss of coke under different atmosphere conditions. In order to more accurately reflect the melting loss behavior of coke under different atmosphere conditions, the coke was ground to a regular cylinder with single particles. Before the experiment, the hanging basket was put into the reaction tube through the hanging wire and the upper end of the hanging wire was hung on the lower hook of the electronic balance to record the weight data of coke in the gasification process. The reaction gas entered the reaction area from the lower part of the reaction tube after passing through the flowmeter, and the reacted gas was discharged from the upper part of the reaction tube. The gas flowmeter could control the flow of each gas, which reached the required conditions of the experiment. Among them, H_2O gas was provided by the gas-distribution system HX-PX04, which was internally equipped with a steam generator. Figure 1 shows the schematic diagram of the comprehensive tester for metallurgical properties of coke. By simulating the composition of blast furnace gas, the coke melting-loss reaction experiment was carried out with different proportions of mixed gas at 1100 °C, and the melting loss rates were calculated according to the mass loss of coke samples. After the melting loss test, the pore parameters, pore-size distribution and microstructure of the samples after reaction were measured.

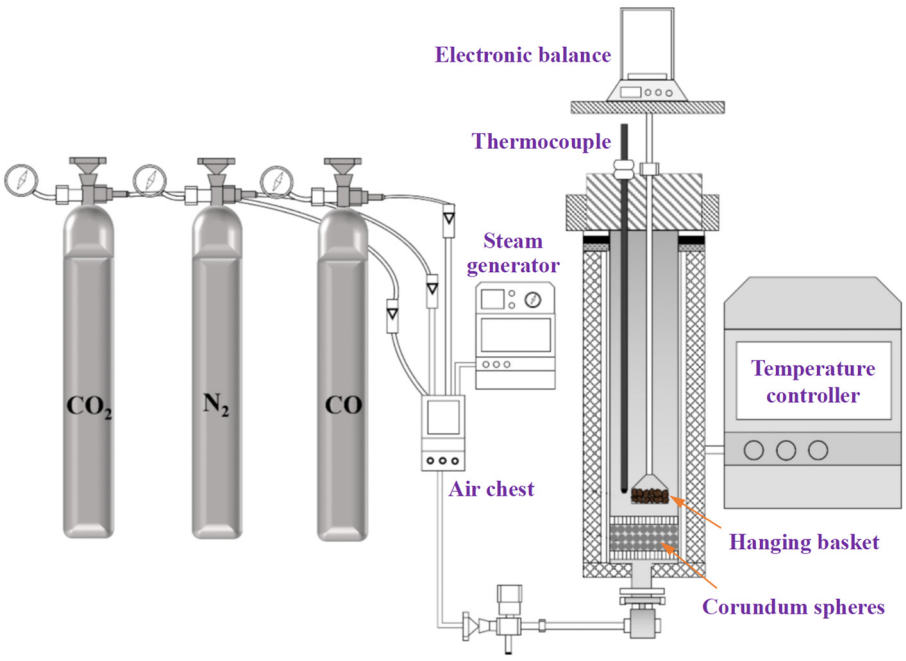

Figure 1. Schematic diagram of a comprehensive tester for coke metallurgical properties.

2.3. Characterization Techniques

The structural parameters of micropores in coke, such as specific surface area, pore volume and average pore diameter, were measured using an automatic surface-area and porosity analyzer with nitrogen as the adsorbent (BET, ASAP2020, Micromeritics Instrument, Norcross, GA, USA). Among them, the analysis range of specific surface area and pore diameter is 0.0005 m^2/g to no upper limit and 3.5–5000 Å, respectively, and the minimum detectable pore volume is 0.0001 cm^3/g. The micromorphology of coke before and after gasification reaction was comprehensively analyzed through the scanning electron microscope with energy-dispersive spectrometer (SEM-EDS, JSM-6510LV, JEOL, Akishima, Tokyo, Japan). A Raman spectrometer (inVia, Renishaw, Wotton-under-Edge, UK) was

adopted to determine the corresponding spectra of coke under different gasification conditions, and the origin software was used to perform peak fitting processing on the spectra to study the evolution law of the microcrystalline structure of coke under different conditions.

3. Results and Discussion

3.1. Influence of CO_2 on Coke Structure

The rather violent carbon melting reaction between CO_2 and coke above 1000 °C is the main reason for the degradation of coke in the blast furnace. The final result of the carbon melting reaction is a large amount of coke matrix damage and strength reduction. However, the damaged coke is seriously pulverized due to its low strength, which reduces the permeability of the blast furnace and affects its smooth running. Therefore, it is necessary to clarify the melting-loss process of coke and CO_2, analyze the changes of micropore structure and physicochemical structure of coke in CO_2 atmosphere, and understand the essence of coke deterioration from the micro level, so as to provide help for improving the coke performance. In this study, by controlling the reaction time of coke and CO_2, the change of specific surface area, pore-size distribution and microstructure of coke under different reaction times was analyzed to study its influence on coke performance.

3.1.1. Effect of CO_2 on Specific Surface Area and Pore-Size Distribution of Coke

The pores on the coke surface are actually the places where coke reacts, and some fine pores are both reaction sites and channels for CO_2 to extend into the coke interior. The reaction of CO_2 in the coke pore is actually carried out on the surface of the pore wall, resulting in the phenomenon of the pore wall thinning in the coke reaction process. When the pore wall is eroded and ruptured, it will connect the closed pores in the coke, causing the change of micropore parameters, and then affect the coke reactivity. The microporous parameters of coke and CO_2 melting-loss reaction at different times are shown in Table 1. It can be seen from Table 1 that when the melting-loss time of coke and CO_2 is less than 3 h, the specific surface area and pore volume of coke increase with the increase in reaction time, while the average pore size decreases. In addition, the increase rate is the most obvious between the melting-loss time of 1 and 2 h. However, when the melting-loss time is further extended to 3 h, the variation trend of coke micropore parameters changes, the specific surface area and pore volume begin to decrease, and the average pore size increases. This indicates that in the initial stage of melting loss, a large number of small gasification substances are generated in the coke and diffuse when coke reacts with CO_2, which promotes the formation of many micropores, so that the amount of micropores increases, resulting in the increase in specific surface area and the decrease in average pore size [29]. When the melting-loss reaction is carried out for 3 h, the coke melts seriously, the matrix is destroyed, the pore wall of coke is broken, and the micropores merge with each other to form macropores, resulting in the decrease in specific surface area and pore volume, and the increase in average pore size. Therefore, it can be determined that there are limiting factors in the specific surface area and pore volume of coke, which are not constant increases.

Table 1. Micropore parameters of coke and CO_2 under different melting-loss times.

Reaction Time (h)	Specific Surface Area (m^2/g)	Pore Volume (cm^3/g)	Average Pore Diameter (nm)
0	9.022	0.01156	17.289
0.5	20.284	0.02119	13.423
1	19.623	0.02194	9.928
2	24.202	0.02536	8.641
3	21.420	0.02432	9.607

The pore-size distribution curve of coke after reaction with CO_2 under different melting loss time is shown in Figure 2, with an enlarged figure between 0–10 nm in the

upper right corner. As can be seen, the pore-size distribution curve of coke samples with the reaction time of 0.5 h is completely below other curves with the pore size of 0–10 nm, and the peak value is the smallest, indicating that the generation of micropores in the coke has not ended when the reaction time is 0.5 h, and the number of micropores in the coke has not reached the peak value. When the pore size is between 2–4 nm, the reaction time of 2 h is significantly higher than that of 3 h either at the peak or at the curve height, indicating that the number of micropores in the coke reaches the peak when the reaction time is 2 h. However, the number of micropores in the coke begins to decrease with the melting loss time further extended to 3 h, which is consistent with the specific-surface-area analysis results. Some scholars [30] also found that the specific surface area of coke was positively correlated with its gasification activity. Under the condition of constant reaction temperature, the coke structure becomes orderly with the increase in reaction time, resulting in a reduction in gasification activity and specific surface area.

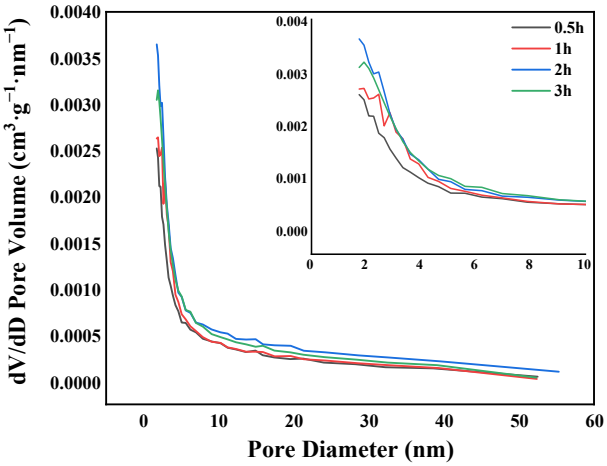

Figure 2. Pore-size distribution of coke and CO_2 under different melting-loss time.

3.1.2. Effect of CO_2 on Microstructure of Coke

Previous studies have proven that coke will react with CO_2 in the blast furnace, and the process of the carbon melting reaction will cause the expansion of pores, which may lead to the spalling of the coke surface matrix and a reduction in particle size. The above change process describes the loose structure and strength reduction of coke from a macro perspective. However, the macroscopic manifestations are all evolved on the microscopic basis, and the essence of coke melting loss can be better understood from the microscopic level. Therefore, it is of great practical significance to study the evolution law of microscopic pores and structures when coke participates in gasification reaction. Scanning electron microscopy (SEM) was used in this study to observe the microstructure of unreacted coke and CO_2 and coke after melting loss at different reaction times, as shown in Figure 3. As can be seen from the yellow underlined area in Figure 3a, the pores on the coke surface before the reaction are round and uniform, and there are few small pores. Although there are visible large pores, the inner wall of the large pores is smooth and tidy, and the pore wall is thick. After 1 h reaction, the number of small pores on the coke surface increases significantly. Figure 3c is an enlarged view of the yellow line area in Figure 3b, from which it is obvious that the inner wall of coke pores is no longer smooth, and the surface of the pore wall becomes rough, which is caused by CO_2 entering into coke and reacting on the pore wall, as well as the reason for the thinning of the pore wall. It can be seen from Figure 3d that the coke is seriously damaged after 3 h of reaction, and a large number of bubbles appear on the surface of the pore wall. Meanwhile, the bubble burst leads to the erosion and penetration of the pore wall, the pores are connected in series, and such small pores are merged with each other to form large pores, resulting in the increase in specific surface area and the further acceleration of the melting-loss reaction.

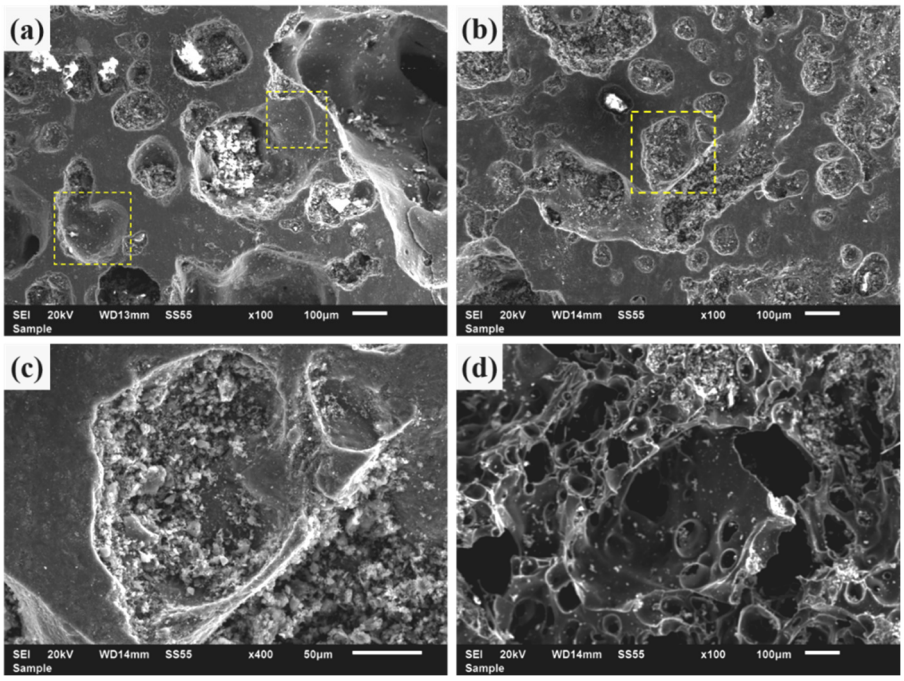

Figure 3. Micromorphology of CO_2 and coke melting loss at different times. (**a**) 0 h; (**b**) 1 h; (**c**) partial enlargement of (**b**); (**d**) 3 h.

3.1.3. Effect of CO_2 on Physicochemical Structure of Coke

Figure 4 shows the peak fitting diagram of the coke Raman spectrum under different reaction times. The influence of time on the coke microstructure in the CO_2 atmosphere is analyzed by the peak area ratio of the fitted peak, and the results of fitting parameters are shown in Table 2. According to the data in this table, the graphitization relative content (I_G/I_{All}) increases first, then decreases and then increases again. However, the variation trend of the disordered structure (I_{D3}/I_G) and unstable structure (I_{D4}/I_G) is opposite to I_G/I_{All}, which decreases first, then increases and decreases again. This is because at the initial stage of the reaction, amorphous carbon atoms inside the coke react with CO_2, the impurity particles on its surface will volatilize, and the disorderly and irregularly layered structure begins to develop towards a regular direction, resulting in the increase in I_G/I_{All} and the decrease in I_{D3}/I_G. When the reaction goes on for 1 h, the chemical bonds of polymer compounds inside the coke begin to break, and the polycondensation reaction taking place between two polymers generates a new polymer compound. At the same time, a large number of sp^2 disordered carbon atoms are left and the defective structure content and unstable structure value (I_{D4}/I_G) increase relatively, which reduces the internal ordering degree and I_G/I_{All} value of coke. As the reaction continues, the melting loss of coke particles gradually reaches the end, the internal polycondensation reaction is basically completed, the residual sp^2 carbon atoms also gradually transform into regular carbon atoms and the value of I_G/I_{All} increases again [31]. It can be inferred that there is a certain connection between the reaction time and the effect of CO_2 on the microstructure of coke. With the extension of the reaction time, the graphitization of coke generally decreases first and then increases, which is related to the sp^2 carbon atoms and amorphous carbon atoms in the coke, mainly depending on the relative content of the two atoms in the coke.

In conclusion, there are similarities and differences between CO_2 and coke reaction modes under different reaction times. In the initial stage, the main performance is that a large number of micropores are generated in the coke, so that the specific surface area increases and the average pore size decreases; in terms of microstructure, the relative content of the disordered structure increases due to a large number of sp^2 disordered carbon atoms remaining in the polycondensation reaction, resulting in a decrease in graphitization degree. At the end of the reaction, the walls of the original micropores and mesopores are

broken, and such pores are connected to form large pores, which reduces the specific surface area and increases the average pore size; at the same time, sp^2 disordered carbon atoms continue to react with CO_2 to transform into an ordered structure, and the graphitized structure increases. In order to achieve the most efficient coke melting-loss rate under the condition of sufficient CO_2, it is necessary to strictly control the performance and particle size of coke.

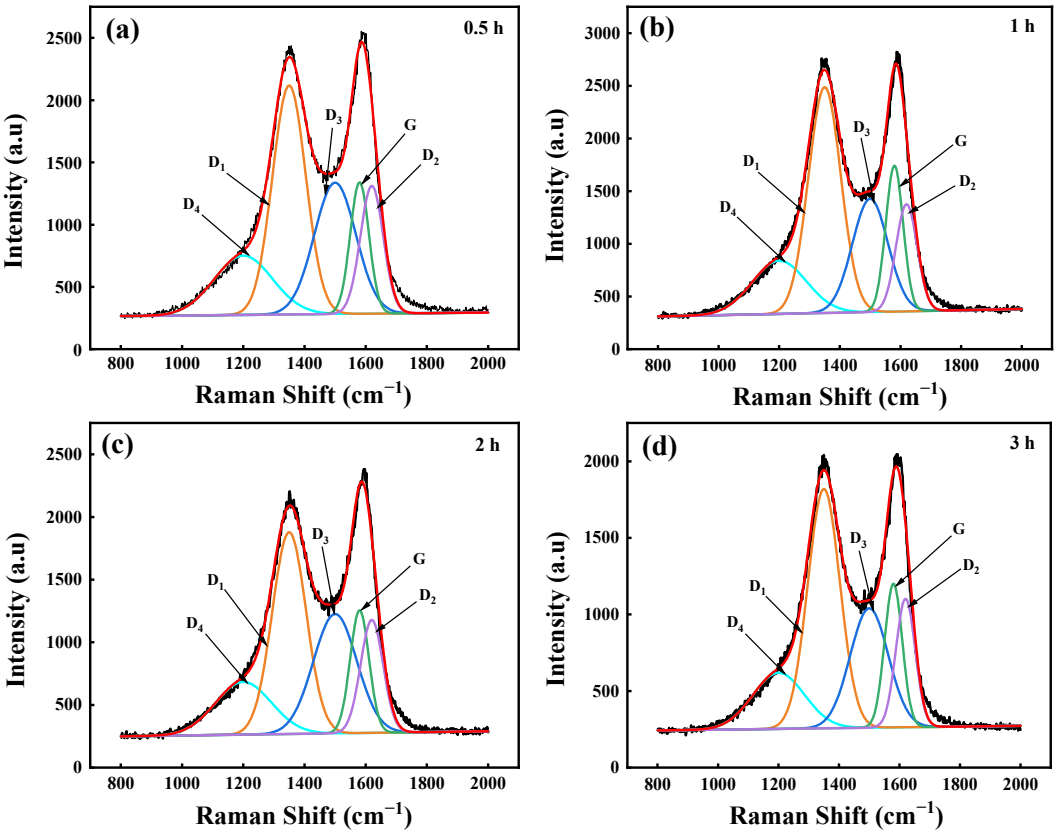

Figure 4. Fitting diagram of Raman peaks of coke and CO_2 at different melting-loss times. (**a**) 0.5 h; (**b**) 1 h; (**c**) 2 h; (**d**) 3 h.

Table 2. Area ratios of fitted peaks for coke and CO_2 at different reaction times (%).

Reaction Time (h)	I_{D1}/I_G	I_{D2}/I_G	I_{D3}/I_G	I_{D4}/I_G	I_G/I_{All}
0	2.83	0.98	1.96	1.15	12.59
0.5	2.90	0.90	1.59	1.14	13.29
1	3.09	1.18	2.21	1.40	11.27
2	3.04	0.98	1.80	1.14	12.57
3	2.95	1.10	2.04	1.17	12.19

3.2. Coinfluence of CO_2 and H_2O on Coke Structure

Coke, as one of the irreplaceable raw materials in the production process of large blast furnaces, must always have some reactivity and postreaction strength in the blast furnace. CO_2 and H_2O coexist in the lower part of the blast furnace shaft, where coke not only reacts with CO_2 in melting loss, but H_2O also participates, both of which have a certain impact on the structure and strength of coke [32]. Therefore, it is of great importance to explore the evolution law of the microparameters of coke in the mixed atmosphere of CO_2 and H_2O to provide a clearer direction for macroresearch.

3.2.1. Coeffect of CO_2 and H_2O on Specific Surface Area and Pore-Size Distribution of Coke

The melting-loss rate of coke under different proportions of CO_2 and H_2O is shown in Table 3. Overall, the coke melting-loss rate is positively correlated with H_2O content. Under the same temperature and reaction time, the mass loss of coke in the condition of 100%H_2O is about 30% more than that of 100%CO_2, which indicates that the reaction capacity between H_2O and coke is higher than that of CO_2. It is reported that the activation energy of adsorption and interfacial reaction under H_2O atmosphere alone is the smallest in the process of carbon melting loss, that is, the most prone to reaction; whereas it is the highest in CO_2 atmosphere, and it is between the two in the mixed atmosphere of CO_2 and H_2O [33]. H_2O molecules react more easily with coke because of its small size, strong expansion capacity and the high activation energy required for the reaction between CO_2 gas molecules and coke.

Table 3. Melting-loss rate of coke under different proportions of CO_2 and H_2O.

Gas Ratio (%)	Prereaction Mass of Coke (g)	Postreaction Mass of Coke (g)	Reaction Time (min)	Reaction Temperature (°C)	Melting-Loss Rate (%)
100%CO_2	8.323	6.642	60	1100	20.19
75%CO_2 + 25%H_2O	7.362	4.999	60	1100	32.09
50%CO_2 + 50%H_2O	7.583	4.568	60	1100	39.76
25%CO_2 + 75%H_2O	7.652	3.971	60	1100	47.42
100%H_2O	7.781	3.695	60	1100	52.51

In order to study the change and distribution of micropores from coke in the mixed atmosphere of CO_2 and H_2O, the samples after reaction were ground and subjected to adsorption and desorption experiments. The variation trends of specific surface area, average pore size and pore volume of coke after reaction under different proportions of CO_2/H_2O are shown in Figure 5. It can be found that with the decrease in CO_2 content and the increase in H_2O content, the specific surface area of coke presents an upward trend, while the average pore size presents a downward trend. Coke generates a certain number of micropores in the early stage of melting-loss reaction, and simultaneously the promotion effect of H_2O molecules accelerates the formation of a large number of micropores in coke, resulting in the increase in specific surface area and the decrease in average pore size. H_2O can promote the formation of micropores, mainly because H_2O molecules are smaller and can enter the micropores in coke to react, and the generated micropores have uniform aperture, which can improve the strength of coke. However, the experimental results show that when the H_2O content in the mixed atmosphere is more than 50%, the specific surface area decreases slightly, and the average pore size increases slightly. Combined with Table 3, it can be seen that at the end of the reaction of coke samples with H_2O content over 50%, the melting-loss rates of both coke samples are up to 47.42% and 52.51%; that is to say, the gasification reaction of coke at this time is particularly intense with the increase in H_2O content. The reaction interface spreads from the surface to the interior of coke, and a large number of micropores are generated in the interior, while the pores on the surface of coke expand and connect with each other, and the number of large pores increases, which leads to the decline in specific surface area and the increase in average pore size.

Figure 6 shows the pore-size distribution of coke after reaction with different proportions of CO_2 and H_2O, and the dot line diagram embedded in the upper right corner of the figure is an enlarged view with abscissa between 0–10 nm in the original figure. The higher the curve in the figure, the more pores corresponding to the aperture. Comparing Figure 6a–f, it can be seen that the pore-size distribution curves participating in the gasification reaction are all higher than those corresponding to the unreacted coke, indicating that the number of micropores in samples participating in melting-loss reaction increases substantially and their distribution is more concentrated compared with unreacted coke. Comparing the peak value of the pore-size distribution curve after gasification reaction, it can be seen that the peak value increases first and then decreases as the H_2O ratio increases,

and reaches the highest value under the condition of 50%CO_2 + 50%H_2O, that is, the overall change trend of micropore content in coke increases first and then decreases. By comparing the pore size corresponding to the peak value of each curve, it is found that the peak value of the pore size is basically at 2 nm before the condition of 50%CO_2 + 50%H_2O, but the pore size corresponding to the peak value shifts to the right after the condition of 50%CO_2 + 50%H_2O, indicating that the pore size has an expanding trend. This is consistent with the results of the specific-surface-area parameter analysis above.

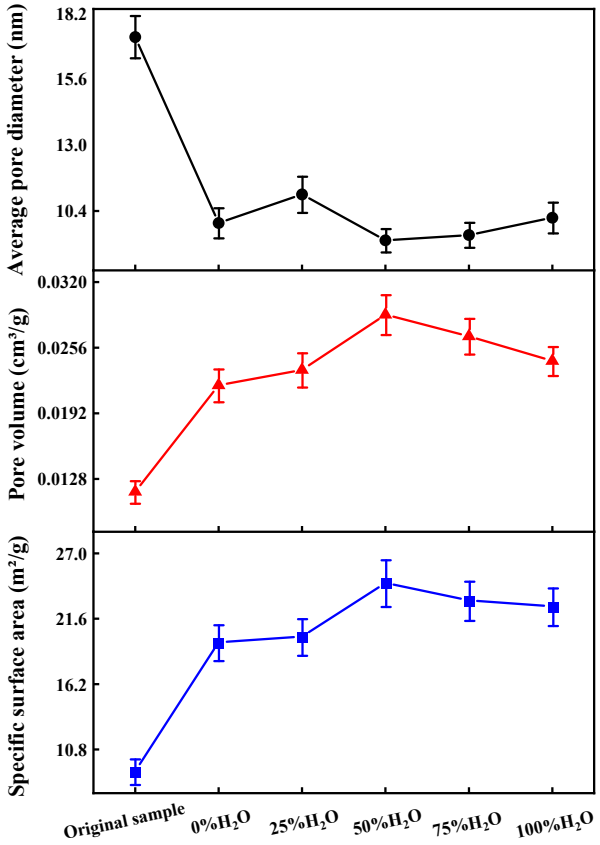

Figure 5. Stomatal parameters of coke reacting with different ratios of CO_2 and H_2O.

3.2.2. Coeffect of CO_2 and H_2O on the Microstructure of Coke

As is known to all, H_2 in the blast furnace will obtain oxygen atoms when participating in the reduction reaction of iron ore, so as to generate H_2O required for the water–gas reaction of coke [24]. With the development of oxygen-rich injection and other technologies, the proportion of H_2 carried in coal gas increases sharply, and so does the content of H_2O in the blast furnace. Therefore, the study on evolution law of micropores and structures during the reaction of coke and H_2O in the blast furnace cannot be ignored. In this study, SEM is used to observe the microstructure of unreacted coke and coke gasification under different proportions of CO_2 and H_2O, as shown in Figure 7. It can be seen that the pores on the surface of unreacted coke are uniform and the number of pores is small. As can be seen from Figure 7b, the melting-loss degree of the coke surface is relatively small under a 100%CO_2 atmosphere, but the number of pores increases and the pore grooves are significantly deepened. When 25%H_2O is added, the number of pores on the coke surface increases significantly and a large number of pores are formed. When the proportion of H_2O reaches 50%, there are a large number of small pores on the coke surface, and at the same time, slender pore grooves appear on the coke surface due to the phenomenon of cross pores, indicating that the coke gradually begins to melt from the outside to the inside. When the proportion of H_2O is further increased to 75%, the coke surface is severely damaged, the pore wall becomes thinner, and the number of large pores occupies most of

the visual interface, through which the coke interior can be directly observed. Finally, the melting loss of the coke surface is basically completed and the gasification reaction begins to expand into the coke interior along the pores when the proportion of H_2O reaches 100%. Therefore, H_2O has a high melting-loss capacity for coke, because H_2O molecules will promote the formation of many micropores in the coke and accelerate the melting loss of the coke internal structure by increasing the reaction area, thus destroying the coke matrix.

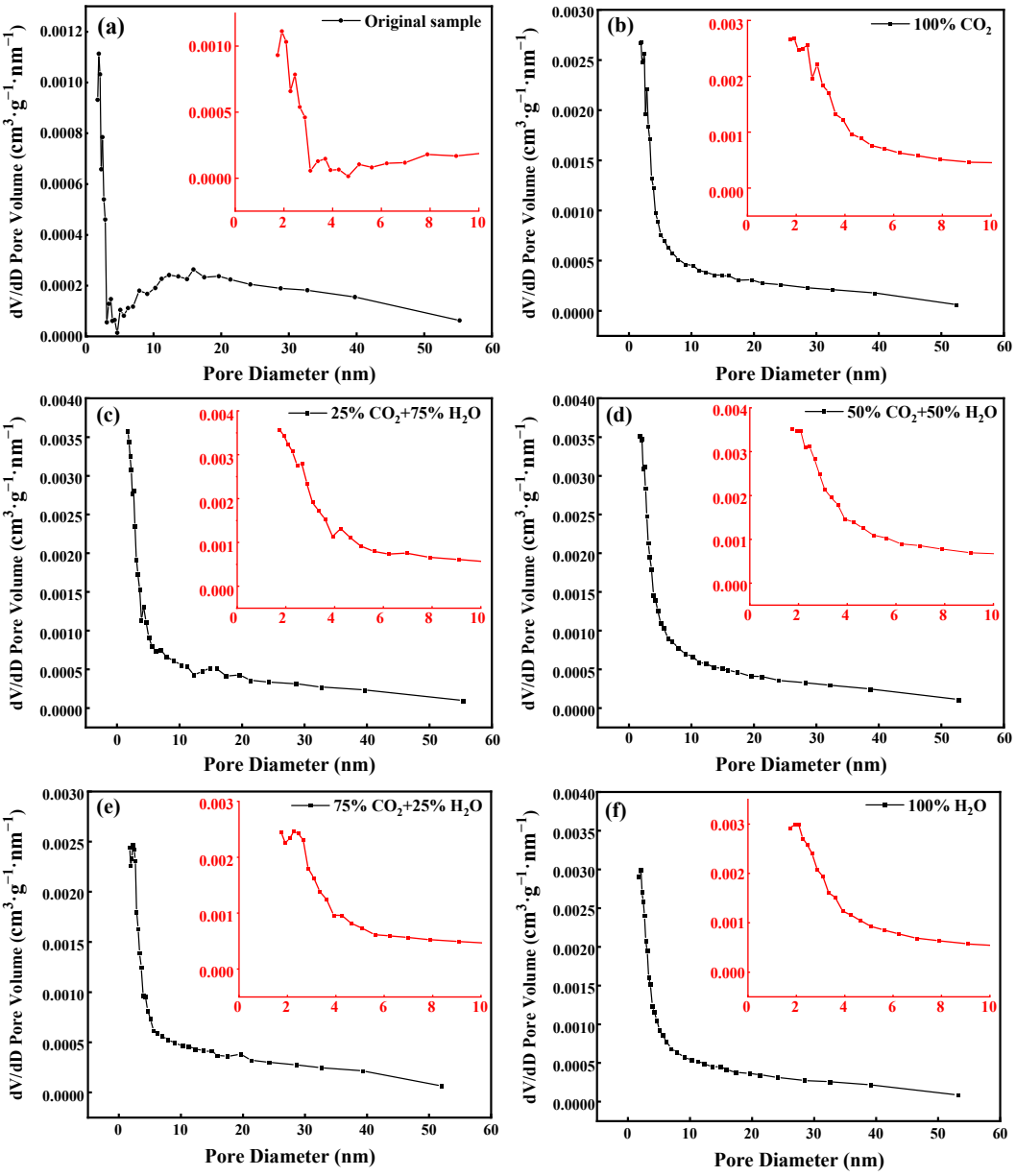

Figure 6. Pore-size distribution after the reaction of CO_2 and H_2O in different proportions. (**a**) Original sample; (**b**) 100%CO_2; (**c**) 25%CO_2 + 75%H_2O; (**d**) 50%CO_2 + 50%H_2O; (**e**) 75%CO_2 + 25%H_2O; (**f**) 100%H_2O.

3.2.3. Coeffect of CO_2 and H_2O on Physicochemical Structure of Coke

Raman spectroscopy is an important means to measure the microstructure changes of carbon-containing materials such as coal coke and characterize the ordering of carbon atoms. Firstly, the D and G peaks in Raman spectra are fitted separately. Then, according to peak position, half-height width (FWHM), peak area and other peak type parameters obtained by peak fitting, the evolution law of coke microcrystalline structure under CO_2

and H_2O conditions is studied. The peak-fitting results of Raman spectra under various conditions are shown in Figure 8 and Table 4.

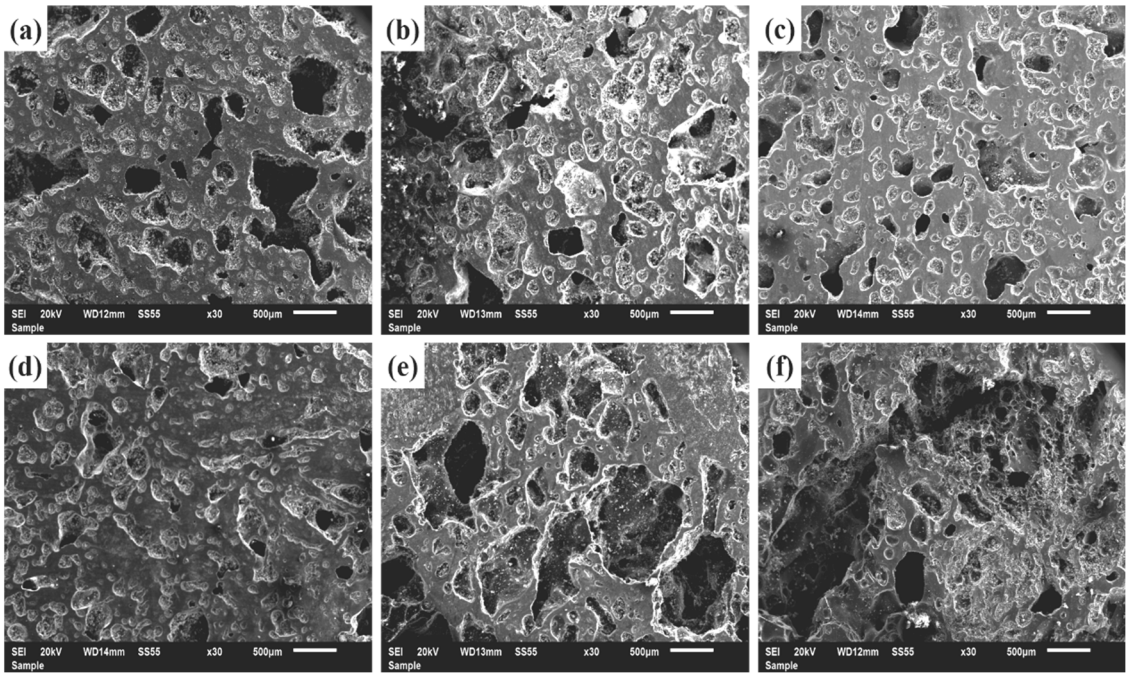

Figure 7. Micromorphology of coke after melting loss under CO_2 and H_2O conditions. (**a**) Original sample; (**b**) 100%CO_2; (**c**) 25%CO_2 + 75%H_2O; (**d**) 50%CO_2 + 50%H_2O; (**e**) 75%CO_2 + 25%H_2O; (**f**) 100%H_2O.

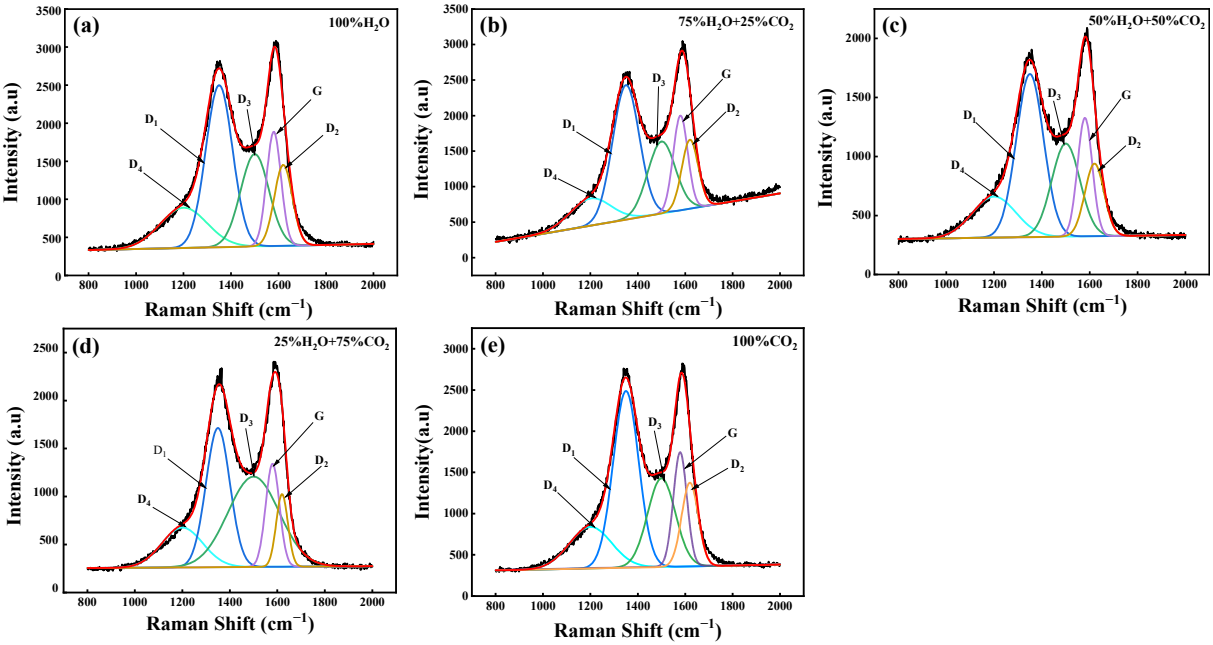

Figure 8. Peak-fitting diagram after the reaction of CO_2 and H_2O. (**a**) 100 %H_2O; (**b**) 75%H_2O + 25%CO_2; (**c**) 50%H_2O + 50%CO_2; (**d**) 25%H_2O + 75%CO_2; (**e**) 100%CO_2.

Table 4. Calculation results of peak area obtained by fitting from Figure 8.

Condition	I_{D1}/I_G	I_{D2}/I_G	I_{D3}/I_G	I_{D4}/I_G	I_G/I_{All}
100%CO_2	3.08	1.17	2.19	1.39	11.33
25%H_2O + 75%CO_2	2.36	0.60	3.24	1.20	11.91
50%H_2O + 50%CO_2	2.54	0.78	1.49	1.02	14.65
75%H_2O + 25%CO_2	2.62	0.86	1.57	1.08	14.02
100%H_2O	2.57	0.79	1.39	0.75	15.38

As can be seen from Table 4, I_G/I_{All} generally increases with the increase in H_2O content, indicating that H_2O plays a positive role in the graphitization degree and ordering of coke, because the carbon atoms in coke's disordered microcrystalline structure are highly active, which is easy for H_2O molecules to react and tend to order. In addition, I_G/I_{All} increases significantly when the proportion of H_2O in the mixed atmosphere reaches 50%, while I_{D3}/I_G and I_{D4}/I_G, which represent the relative content of the disordered structure and unstable structure, respectively, decrease accordingly, indicating that the reaction between the disordered microcrystalline structure and H_2O is more significant when the content of H_2O is higher. This is because CO_2 molecules are larger; H_2O molecules can more easily enter the coke interior and cause a gasification reaction with the disordered structure compared with CO_2 molecules, so the disordered structure changes to the ordered structure, resulting in the increase in I_G/I_{All}. This is also why H_2O gasification reactivity with coke is higher than CO_2. Other studies [22] have also shown that in the mixed atmosphere of CO_2 and H_2O, there will be an obvious interaction between coke and their cogasification process when the proportion of H_2O is greater than or equal to 50%, promoting the coke structure to further tend to be ordered.

4. Conclusions

The design and optimization of the new-generation ironmaking process centering on blast furnaces to realize the collaborative continuous and dynamic order of the whole ironmaking process will be the key research direction and breakthrough of future ironmaking technology innovation. In this study, the gasification reaction of coke in a blast furnace was simulated, and the evolution laws of pore-size distribution, micromorphology and physicochemical structure of coke under CO_2, CO_2 and H_2O atmospheres were characterized via specific surface area and porosity adsorption instrument, scanning electron microscopy and Raman spectroscopy. The following conclusions were drawn:

1. In the CO_2 atmosphere, the specific surface area and pore volume of coke increased first and then decreased with the reaction time increasing from 0 to 3 h, and both reached their maximum values at 2 h of reaction, which were 24.202 m^2/g and 0.02536 cm^3/g, respectively, while the average pore size first decreased from 17.289 to 8.641 nm and then slightly increased to 9.607 nm. Similarly, the number of micropores in coke increased first and then decreased as the reaction time increased, which was consistent with the change trend of specific surface area.
2. During the melting loss of CO_2 and coke, the relative content of graphitization (I_G/I_{All}) first increased, then decreased and then increased again, with a value range of 11.27%–13.29%. However, the content of disordered structure (I_{D3}/I_G) and unstable structure (I_{D4}/I_G) had the opposite trend with I_G/I_{All}, with the value range of 1.80%–2.21% and 1.14%–1.40%, respectively. It meant that coke still tended to be more orderly with the increase in time.
3. In the mixed atmosphere of CO_2 and H_2O, the specific surface area of coke generally increased with the increase in the H_2O content, and its maximum value was 24.573 m^2/g. However, when the proportion of H_2O exceeded 50%, the specific surface area decreased slightly, and the pore-size value corresponding to the peak value in the pore-size distribution curve deviated to the right.

4. With the increase in H_2O content, I_G/I_{All} increased gradually. When H_2O content in the mixed atmosphere exceeded 50%, I_G/I_{All} increased significantly, and but the I_{D3}/I_G and I_{D4}/I_G values decreased correspondingly. It indicated that the reaction between the disordered microcrystalline structure and H_2O was more significant when the content of H_2O was higher, which accelerated the transition from the disordered structure to the ordered structure.

Author Contributions: The manuscript was written through contributions of all authors. Y.Z. and J.Y. performed the resources, writing—review and editing, supervision and data curation.; H.W. performed the SEM, EDS and LSCM measurements; L.Y. performed the surface cleaning and sample polishing; S.C. performed sample preparation and image processing. All authors have read and agreed to the published version of the manuscript.

Funding: This work was supported by the National Key R&D Program of China (2017YFB0603800 & 2017YFB0603802) and Anhui Province Science Foundation for Excellent Young Scholars (2108085Y19).

Institutional Review Board Statement: Not applicable.

Informed Consent Statement: Not applicable.

Data Availability Statement: Not applicable.

Conflicts of Interest: The authors declare no conflict of interest.

References

1. Gupta, S.; Dubikova, M.; French, D.; Sahajwalla, V. Effect of CO_2 gasification on the transformations of coke minerals at high temperatures. *Energy Fuels* **2007**, *21*, 1052–1061. [CrossRef]
2. Wang, J.; Zhang, Y.; Cui, K.; Fu, T.; Gao, J.; Hussain, S.; AlGarni, T.S. Pyrometallurgical recovery of zinc and valuable metals from electric arc furnace dust—A review. *J. Clean. Prod.* **2021**, *298*, 126788. [CrossRef]
3. Gupta, S.; Sahajwalla, V.; Chaubal, P.; Youmans, T. Carbon structure of coke at high temperatures and its influence on coke fines in blast furnace dust. *Metall. Mater. Trans. B* **2005**, *36*, 385–394. [CrossRef]
4. Gornostayev, S.; Härkki, J. Mineral matter crystallization and crack formation in tuyere coke. *Fuel* **2006**, *85*, 1047–1051. [CrossRef]
5. Cui, K.K.; Mao, H.B.; Zhang, Y.Y.; Wang, J.; Wang, H.; Tan, T.B.; Fu, T. Microstructure, mechanical properties, and reinforcement mechanism of carbide toughened ZrC-based ultra-high temperature ceramics: A review. *Compos. Interfaces* **2022**, *29*, 729–748. [CrossRef]
6. Sakurovs, R.; French, D.; Grigore, M. Effect of the NSC reactivity test on coke mineralogy. *Int. J. Coal Geol.* **2012**, *94*, 201–205. [CrossRef]
7. Grigore, M.; Sakurovs, R.; French, D.H.; Sahajwalla, V. Effect of carbonisation conditions on mineral matter in coke. *ISIJ Int.* **2007**, *47*, 62–66. [CrossRef]
8. Lee, W.; Lee, Y. Internal gas pressure characteristics generated during coal carbonization in a coke oven. *Energy Fuel* **2001**, *15*, 618–623. [CrossRef]
9. Shen, F.L.; Gupta, S.; Liu, Y.; Meng, Q.B.; French, D.; Sahajwalla, V. Effect of reaction conditions on coke tumbling strength, carbon structure and mineralogy. *Fuel* **2013**, *111*, 223–228. [CrossRef]
10. Wang, J.; Zhang, Y.Y.; Yu, L.H.; Cui, K.K.; Fu, T.; Mao, H.B. Effective separation and recovery of valuable metals from waste Ni-based batteries: A comprehensive review. *Chem. Eng. J.* **2022**, *439*, 135767. [CrossRef]
11. Wu, S.Y.; Zhang, X.; Gu, J.; Wu, Y.Q.; Gao, J.S. Interactions between carbon and metal oxides and their effects on the carbon/CO_2 reactivity at high temperatures. *Energy Fuels* **2007**, *21*, 1827–1831. [CrossRef]
12. Kawakami, M.; Kanba, H.; Sato, K.; Takenaka, T.; Gupta, S.; Chandratilleke, R.; Sahajwalla, V. Characterization of thermal annealing effects on the evolution of coke carbon structure using Raman spectroscopy and X-ray diffraction. *ISIJ Int.* **2006**, *46*, 1165–1170. [CrossRef]
13. Heikkilä, A.M.; Koskela, A.M.; Iljana, M.O.; Lin, R.; Bartusch, H.; Heikkinen, E.; Fabritius, T.M.J. Coke gasification in blast furnace shaft conditions with H_2 and H_2O containing atmospheres. *Steel Res. Int.* **2020**, *92*, 2000456. [CrossRef]
14. Danloy, G.; Delinchant, J.; Janhsen, U.; Lectard, E. New characterisation tests of the coke behaviour at high temperature. *Revue Métallurgie* **2009**, *106*, 48–59. [CrossRef]
15. Tian, Y.; Li, G.Y.; Zhang, H.; Wang, J.P.; Ding, Z.Z.; Guo, R.; Cheng, H.; Liang, Y.H. Molecular basis for coke strength: Stacking-fault structure of wrinkled carbon layers. *Carbon* **2020**, *162*, 56–65. [CrossRef]
16. Li, K.J.; Zhang, J.L.; Sun, M.M.; Jiang, C.H.; Wang, Z.M.; Zhong, J.B.; Liu, Z.J. Existence state and structures of extracted coke and accompanied samples from tuyere zone of a large-scale blast furnace. *Fuel* **2018**, *225*, 299–310. [CrossRef]

17. Chapman, M.W.; Monaghan, B.J.; Nightingale, S.A.; Mathieson, J.G.; Nightingale, R.J. Formation of a mineral layer during coke dissolution into liquid iron and its influence on the kinetics of coke dissolution rate. *Metall. Mater. Trans. B* **2008**, *39*, 418–430. [CrossRef]
18. Chapman, M.W.; Monaghan, B.J.; Nightingale, S.A.; Mathieson, J.G.; Nightingale, R.J. Observations of the mineral matter material present at the coke/iron interface during coke dissolution into iron. *ISIJ Int.* **2007**, *47*, 973–981. [CrossRef]
19. Petersen, I.; Werther, J. Experimental investigation and modeling of gasification of sewage sludge in the circulating fluidized bed. *Chem. Eng. Process. Process Intensif.* **2005**, *44*, 717–736. [CrossRef]
20. Li, J.; Kuang, S.B.; Jiao, L.L.; Liu, L.L.; Zou, R.P.; Yu, A.B. Numerical modeling and analysis of hydrogen blast furnace ironmaking process. *Fuel* **2022**, *323*, 124368. [CrossRef]
21. Sun, Z.; Lin, X.; Li, P.; Liang, Y.H. Influence of solution loss reaction temperature to the thermal properties of high reactivity coke. *Fuel Chem. Process.* **2014**, *45*, 8–12.
22. Zhao, Q.Q.; Xue, Q.G.; Yu, X.F.; Wang, H.; Wang, J.S. Study on solution loss reaction kinetics of coke with H_2O and CO_2. *Chin. J. Process Eng.* **2012**, *12*, 789–795.
23. Gupta, S.; Ye, Z.Z.; Kanniala, R.; Kerkkonen, O.; Sahajwalla, V. Coke graphitization and degradation across the tuyere regions in a blast furnace. *Fuel* **2013**, *113*, 77–85. [CrossRef]
24. Guo, W.T.; Wang, J.S.; She, X.F.; Xue, Q.G.; Guo, Z.C. Pore structure and high-temperature compressive strength of gasified coke with CO2 and steam. *J. Fuel Chem. Technol.* **2015**, *43*, 654–662.
25. Zhang, Y.Y.; Yu, L.H.; Fu, T.; Wang, J.; Shen, F.Q.; Cui, K.K. Microstructure evolution and growth mechanism of Si-$MoSi_2$ composite coatings on TZM (Mo-0.5Ti-0.1Zr-0.02C) alloy. *J. Alloys Compd.* **2022**, *894*, 162403. [CrossRef]
26. Zhang, Y.Y.; Yu, L.H.; Fu, T.; Wang, J.; Shen, F.Q.; Cui, K.K.; Wang, H. Microstructure and oxidation resistance of Si-$MoSi_2$ ceramic coating on TZM (Mo-0.5Ti-0.1Zr-0.02C) alloy at 1500 °C. *Surf. Coat. Technol.* **2022**, *431*, 128037. [CrossRef]
27. Fu, T.; Cui, K.K.; Zhang, Y.Y.; Wang, J.; Shen, F.Q.; Yu, L.H.; Qie, J.M.; Zhang, X. Oxidation protection of tungsten alloys for nuclear fusion applications: A comprehensive review. *J. Alloys Compd.* **2021**, *884*, 161057. [CrossRef]
28. Zhang, Y.Y.; Fu, T.; Yu, L.H.; Shen, F.Q.; Wang, J.; Cui, K.K. Improving oxidation resistance of TZM alloy by deposited Si-$MoSi_2$ composite coating with high silicon concentration. *Ceram. Int.* **2022**, *48*, 20895–20904. [CrossRef]
29. Yang, S.P.; Wang, C.; Dong, J.; Wang, C.; Ji, Z.Z.; Pang, J.K. Effect of CO_2 on high temperature gasification and microstructure analysis of coke. *J. Iron Steel Res.* **2019**, *1*, 24–30.
30. Hu, J.; Kong, F.S.; Zhao, X.M.; Song, J.H.; Zhang, J.L. Effect of blast furnace coal injection on thermal property of coke. *J. China Coal Soc.* **2003**, *4*, 419–422.
31. Liu, X.Q.; Liu, Y.H.; Lv, Q. Study on structure evolution characteristics of Zhundong coal char during devolatilization in $O_2/H_2O/CO_2$ atmospher. *Therm. Power Gener.* **2022**, *51*, 139–149.
32. Xu, R.S.; Dai, B.W.; Wang, W.; Schenk, J.; Bhattacharyya, A.; Xue, Z.L. Gasification reactivity and structure evolution of metallurgical coke under H_2O/CO_2 atmosphere. *Energy Fuels* **2018**, *32*, 1188–1195. [CrossRef]
33. Zhao, J.; Zuo, H.B.; Ling, C.; Guo, W.T.; Wang, J.S.; Xue, Q.G. Microstructure evolution of coke under CO_2 and H_2O atmospheres. *J. Iron Steel Res. Int.* **2020**, *27*, 743–754. [CrossRef]